

Use of a plane jet for flow-induced noise reduction of tandem rods

This content has been downloaded from IOPscience. Please scroll down to see the full text.

2016 Chinese Phys. B 25 064301

(<http://iopscience.iop.org/1674-1056/25/6/064301>)

View [the table of contents for this issue](#), or go to the [journal homepage](#) for more

Download details:

IP Address: 134.226.144.29

This content was downloaded on 19/01/2017 at 10:25

Please note that [terms and conditions apply](#).

You may also be interested in:

[The characteristics of the Aeolian tone radiated from two-dimensional cylinders](#)

Hajime Fujita

[Aerodynamic noise reduction by pile fabrics](#)

Masaharu Nishimura and Tomonobu Goto

[A review of diagnostic studies on jet-noise sources and generation mechanisms of subsonically convecting jets](#)

Takao Suzuki

[Pulse-burst PIV in a high-speed wind tunnel](#)

Steven Beresh, Sean Kearney, Justin Wagner et al.

[Reduction of airfoil trailing edge noise by trailing edge blowing](#)

T Gerhard, S Erbslöh and T Carolus

[Flow structure around a finite circular cylinder embedded in various atmospheric boundary layers](#)

Cheol-Woo Park and Sang-Joon Lee

[Particle image velocimetry technique measurements of the near wake behind a cylinder-pair of unequal diameters](#)

Y Y Gao, Xikun Wang, D S Tan et al.

[Bluff body flow and vortex—its application to wind turbine](#)

Yuji Ohya

Use of a plane jet for flow-induced noise reduction of tandem rods*

Kun Zhao(赵鲲)^{1,2}, Xi-xiang Yang(杨希祥)^{1,†}, Patrick N Okolo^{2,3}, Wei-hua Zhang(张为华)¹, and Gareth J Bennett²

¹College of Aerospace Science and Engineering, National University of Defence Technology, Changsha 410073, China

²Department of Mechanical and Manufacturing Engineering, Trinity College Dublin, University of Dublin, Dublin 2, Dublin, Ireland

³Energy and Power Technology Division, Department of Mechanical Engineering, University of Nigeria, Nsukka, Nigeria

(Received 27 September 2015; revised manuscript received 17 January 2016; published online 20 April 2016)

Unsteady wake from upstream components of landing gear impinging on downstream components could be a strong noise source. The use of a plane jet is proposed to reduce this flow-induced noise. Tandem rods with different gap widths were utilized as the test body. Both acoustic and aerodynamic tests were conducted in order to validate this technique. Acoustic test results proved that overall noise emission from tandem rods could be lowered and tonal noise could be removed with use of the plane jet. However, when the plane jet was turned on, in some frequency range it could be the subsequent main contributor instead of tandem rods to total noise emission whilst in some frequency range rods could still be the main contributor. Moreover, aerodynamic tests fundamentally studied explanations for the noise reduction. Specifically, not only impinging speed to rods but speed and turbulence level to the top edge of the rear rod could be diminished by the upstream plane jet. Consequently, the vortex shedding induced by the rear rod was reduced, which was confirmed by the speed, Reynolds stress as well as the velocity fluctuation spectral measured in its wake. This study confirmed the potential use of a plane jet towards landing gear noise reduction.

Keywords: plane jet, tandem rods, flow-induced noise reduction, vortex shedding

PACS: 43.58.+z, 47.32.cb, 43.50.+y

DOI: 10.1088/1674-1056/25/6/064301

1. Introduction

Popularity of air travel has dramatically increased over the last few decades and aircraft noise is currently a major concern in aeronautical industries. Due to high bypass ratio configuration,^[1,2] engine noise has been significantly reduced, making airframe noise the principal culprit for annoyance, especially in airport proximity. For this reason, airframe noise reduction, particularly the main contributor — landing gear — should be an essential consideration in the design of new commercial aircraft.^[3] To reduce landing gear noise, a few techniques have been proposed and implemented. The fundamental idea behind current techniques such as fairings^[4,5] and wheel hub caps^[6] is to cover the landing gear with aerodynamically refined components. However, this form of passive control is limited for practical reasons, e.g., impeding visual inspection and maintenance of the landing gear. Therefore, proposal and validation of new ideas are still necessary.

In terms of the overall sound pressure level (OASPL) of noise generated by landing gear, contribution of different components depends on specifics of the actual design. Studies on flow-induced noise of various objects^[7–11] have been conducted. Overall speaking, there is an approximation, i.e., sixth power law, which has been widely applied to the noise level prediction. Specifically, OASPL of the landing gear noise (component) is in direct ratio to the sixth power of local flow speed. In other words, total noise emission can be lowered by reducing local flow speed. Apart from the noise associated with direct impinging of main-flow, another important noise

generation mechanism is that when turbulent wake from the upstream gear component interacts with the downstream component, which leads to excess aerodynamic noise.^[12] Previous studies^[12] concluded that interaction noise produced by the turbulent eddy of strength near a compact rigid body has a positive function of eddy convection velocity and correlation scale of the turbulence. Accordingly, the key to reducing the interaction noise is to reduce both convection velocity and turbulent stress in the wake flow that impinges on downstream components.^[13]

In this study, a plane jet is proposed to reduce the flow-induced noise. Tandem rods were used as the test body because turbulent wake from upstream rods can cause more noise emission when it impinges on the rear rod. The plane jet can provide a good shield to tandem rods and can be simplified as a two-dimensional (2D) system to find the location of the rods. To be more specific, the idea of tandem rods noise reduction using a plane jet is to apply an upstream blowing air to deflect flow impinging the rods so that aerodynamic noise can be reduced. Both acoustic and aerodynamic measurements were performed, based on which relevant conclusions were drawn and noise reduction was firmly validated, particularly the noise generated due to interaction between the rear rod and wake from the front rod.

2. Apparatus and procedure

Figure 1 illustrates the entire experimental rig utilized in the test, which consists of an open-jet wind tunnel, a plane

*Project partially supported by the European Union FP7 CleanSky Joint Technology Initiative “ALLEGRA” (Grant No. 308225).

†Corresponding author. E-mail: nkyangxixiang@163.com

jet system, a beam-forming array and the test body mentioned above. Also, techniques such as PIV and hot-wire were used for the measurements.

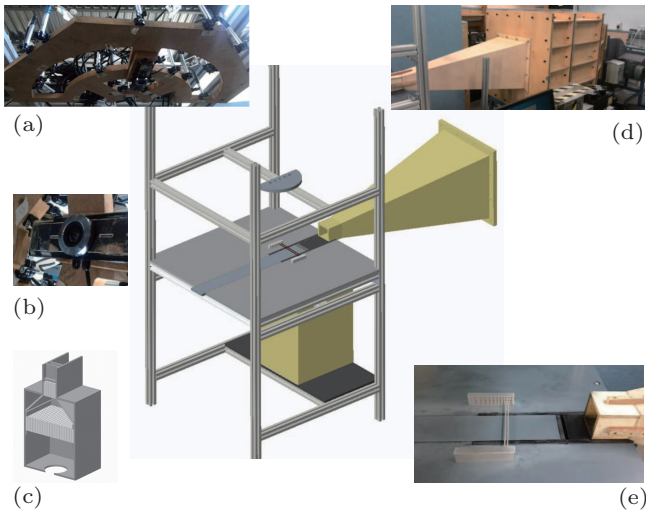


Fig. 1. (color online) Schematic diagram of experimental facilities: (a) Microphone array; (b) beam-forming camera; (c) plane jet plenum; (d) main-flow nozzle and the plenum; (e) rods set-up.

2.1. Wind tunnel and the plane jet blower

As shown in Fig. 1(d), measurements were performed in a low-speed open-jet wind tunnel. Specifically, the wind tunnel is powered by a 5.5-kW centrifugal blower. Between the blower and the nozzle there is a cubic plenum connected, the size of which is 800 mm×800 mm×800 mm. In order to uncouple the flow from the blower and ensure a low turbulence intensity, a series of honeycomb layers are subsequently installed inside the plenum. As for the nozzle, length is 1000 mm and the square outlet size is 75 mm×75 mm. One horizontal end-plate is mounted and flush with the lower side of the nozzle, providing a three-quarter open test section for the measurement.

The plane jet blowing system includes a 2.2-kW centrifugal blower and a cubic plenum as well as a nozzle, shown in Fig. 1(c). In order to facilitate movement of the plenum, a hose is linked from the blower outlet to the plenum bottom, on which there is a hole for connection. Height of the plenum is 540 mm and size of the horizontal section is 424 mm×424 mm. Likewise, two layers of honeycomb with hexagonal grid (6-mm edge length) are installed to uncouple the flow from the blower and acquire a low turbulence intensity inside the plenum. In addition, baffles are added to minimize recirculation. As for shape of the nozzle on top of the plenum, it is fixed to be rectangular with a constant length of 100 mm and changeable width. In the test, the nozzle was set to be flush with the wind tunnel end-plate, and the width was chosen to be 10 mm. In addition, velocity of both main-flow coming from the wind tunnel and the plane jet could be controlled by adjusting the blower inlet area.

2.2. Test object

As mentioned earlier, tandem rods were used as the test object. Radius of the rods, D is 4 mm and both of them are polished (Fig. 2) to eliminate effects from roughness of the surface. For gap width L , particular values of L/D may lead to different flow regimes. For example,^[14] when $1.1-1.3 < L/D < 3.5-3.8$, free shear layers that get separated from the front rod may reattach alternately, permanently or intermittently onto the rear rod. Therefore, vortex shedding takes place mainly behind the rear rod. In this study, this configuration was adopted. More precisely, values of L/D in the study were 2, 2.5, 3, and 3.5.



Fig. 2. (color online) Tandem rods used in the test.

As shown in Fig. 1(e), tandem rods were supported by tow blocks with a series of tubes, which could help adjust height to the end-plate and gap width between tandem rods. As for the height and the gap, both would be chosen based on PIV results hereinafter.

2.3. Acoustic measurement

Beam-forming is an array-based measurement technique for sound source localization. It has become a standard method for spatial noise mapping. In this study, a planar semi-circular array with a camera was built, shown in Fig. 1(a) and Fig. 1(b). The array has a diameter of 600 mm and an irregular pattern of 25 microphones. On account of the beam-forming camera, the noise localization can be superimposed on a real photograph background. Moreover, this pattern can reduce typical spatial aliasing of the regular array. In this study, beam-forming in the time domain with diagonal deletion was used with 1/3 octave band filter. Mathematical theory can be found in Refs. [15] and [16]. Signals from microphones were amplified before being simultaneously sampled using the National Instrument DAQ system. Sampling rate and sampling time were set to be 80 kHz and 6 s respectively. All microphones were calibrated before being used. To validate the noise localization, an array calibration technique using one small speaker was conducted. Explicitly, one small speaker was differently positioned on the end-plate, generating broadband noise and therefore localized by the beam-forming array. Results are shown in Fig. 3, noise contour superimposed on background

pictures visualized the sound pressure level (SPL) on the end-plate from the top view and the contour was normalised by subtracting the maximum SPL of each case to highlight source localization. As can be seen, the peak localises the speaker movement very well.

Additionally, as the microphone array was placed out of main-flow, the refraction due to density gradient caused by the shear layer could affect the directivity of sound propagation as well as noise localization accuracy. However, since no directivity measurement was conducted and the beam-forming array was only 493 mm high to the end-plate in this study, no shear layer refraction corrections were performed.

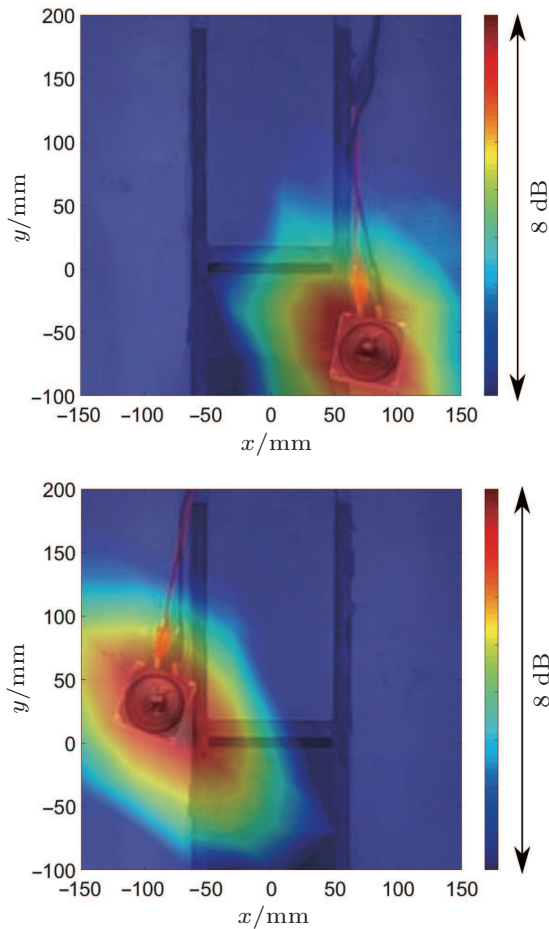


Fig. 3. (color online) Beam-forming calibration.

2.4. Aerodynamics measurement

2.4.1. Particle image velocimetry

Particle Image Velocimetry, i.e., PIV, is an optical flow measurement that is capable of providing quantitative flow parameters. In the study, the flow structure without rods were visualized by DaVis low-speed PIV system. Specifically, the DaVis Flowmaster 3 CCD camera was parallelly assembled beside the end-plate, capturing the images with a Nd:YAG laser pulsing. As illustrated in Fig. 4, the green laser sheet, i.e., the measurement plane was generated through the sheet former lens after a mirror for reflection of the laser beam. The

plane was projected in the centre of the flow from the top view. For each flow case, 2000 image pairs were captured to acquire mean flow field and the time between two pairs was 10 μ s. Phantom 135 smoke system was used to inject seeding to the main-flow. As for the vector field calculation, the interrogation window using 128×128 pixels with a 50% overlap was adopted.

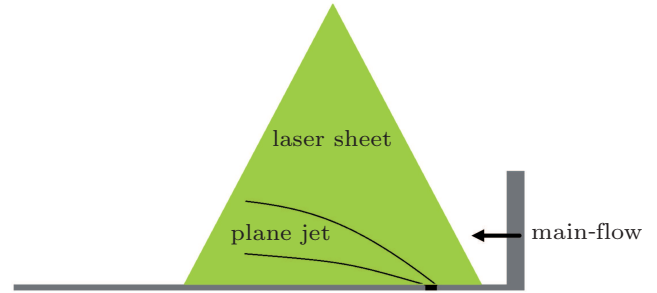


Fig. 4. (color online) PIV measurement plane.

2.4.2. Constant temperature anemometer

The constant temperature anemometer (CTA), i.e., hot-wire anemometer, uses a very fine wire electrically heated up to some temperature above the ambient. The air flowing passing the wire has a cooling effect (forced convection) and a relationship can be obtained between resistance of the wire and flow speed. Essentially, the key to this technique is based on the principle of heat transfer and its effects on the resistance of the wire.^[17] Advantages of the hot-wire anemometry can be summarized as high frequency response and high data rates, which are very helpful to measure Reynolds stress and fluctuating velocity spectrum. In this experiment, the Dantec CTA system was utilized to do the data acquisition and the probe was single-wire Dantec 55P15, which can measure one velocity component in three-dimensional (3D) system. In the test, the stream-wise component, i.e., u in x direction was measured. In addition, due to ambient temperature of the calibration and in different tests, temperature correction was applied for the measurement.^[18]

Due to limitation of experimental instrumentation, it is impossible to measure the real impinging speed and Reynolds stress on the test body surfaces. As a consequence, some certain test sections were chosen to perform the measurement, which could reflect flow variation.

Figure 5 schematically illustrates measurement sections (dotted red line), which starts from line A and ends at line B. Line A is the centreline of rod section and parallel to the end-plate. Line B was $3D/2$ higher than line A. The entire measurement was conducted inside the centre plane of the open-jet tunnel. The upstream section was in the middle of the gap between two rods, which approximately measured the impinging speed and Reynolds stress to the rear rod. The downstream

section was $3D/2$ behind the rear rod, which enables measurement of the wake behind the rear rod.

In the tests, a hot-wire support tube was mounted on a vertical traverse connected to a servo motor (Animatics SM23165D). In addition, the samples were taken every $D/8$ in each section. As for Reynolds stress, since the single-wire

hot-wire could only measure the velocity in one dimension, the stream-wise component was chosen, that is, the $u'u'$, which also dominated over the other stress terms. The real test set-up is shown in the following Fig. 5(b), and the thermal probe set inside the downstream was used to perform the thermal correction.

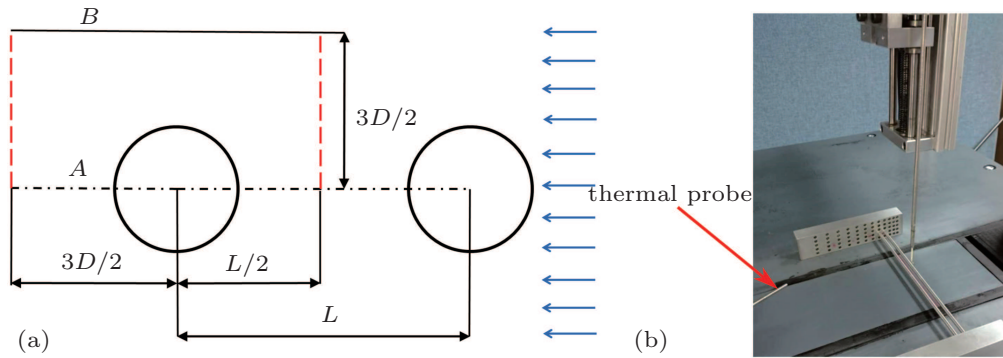


Fig. 5. (color online) Hot-wire measurement.

2.5. Testing campaign and conditions

During the test, speed of the main-flow and the plane jet were controlled to be 50 m/s (U_∞) and 55 m/s (U_j). Three flow regimes were chosen to facilitate comparison. As schematically shown in Fig. 6, “background noise” represents the regime that main-flow is actively switched on without the rods and the plane jet. Meanwhile, the plane jet orifice is sealed to avoid possible cavity noise induced by main-flow; “NoPJ” represents the regime that main-flow is on with rods, but no plane jet; “PJ” represents the regime that the plane jet is turned on compared to “NoPJ”.

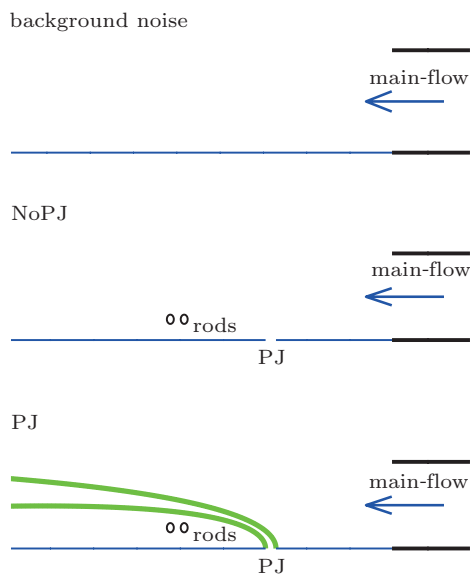


Fig. 6. (color online) Schematic diagram of the test campaign.

Previous studies^[19–21] demonstrated that the flow pattern behind the jet has complicated structures, and there is a low

speed area behind it. Since the aerodynamic noise is in direct ratio to the 6th power of the local flow speed around the bluff-body components, it is best to put the rods in the low speed area. In this study, PIV experiment was performed to seek the location for rods.

Figure 7 is PIV results on the flow speed field with vectors illustrating flow direction. The Y axis represents the height referred to the end-plate and normalized by D . The X axis represents the stream-wise length normalized by W . In addition, the origin was located in the centre of the slot. As shown in Fig. 7(a), a stream-wise low velocity area exists due to the boundary layers, which has a height of approximately $2h/D$. More studies on boundary layers of cross-flow can be found in Refs. [22] and [23]. Meanwhile, over the $18h/D$, there is a shear layer with high speed gradient, which can result in noise refraction mentioned earlier. Rods should be lower than the shear layer flow and higher than the boundary layer, both of which do not exist when the landing gear interacts with the coming flow, in order to approach real flight conditions as much as possible. More importantly, when the plane jet is turned on, a low speed area is highly preferred as it will contribute to the noise reduction. Therefore, the primary rod was simply chosen to be centred at $(10, 2.5)$ in terms of $2D$ view. Figure 8 shows the velocity profile normalized by U_∞ at the section $x = 10$, in which the two circles represented the rods (the profile was acquired without rods). The front rod was centred at $(10, 2.5)$. As is clearly depicted, velocity can be significantly lowered with the plane jet. In other words, the plane jet has great potential to reduce the landing gear noise.

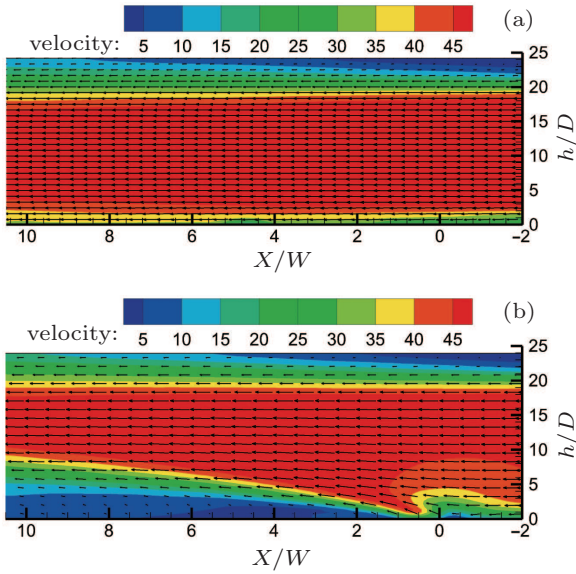


Fig. 7. (color online) Flow velocity field for case (a) without plane jet and (b) with plane jet.

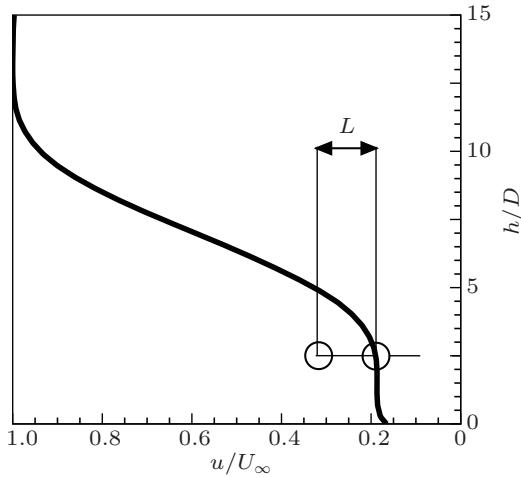


Fig. 8. Velocity profile for the impinging velocity.

3. Results and discussions

In this section, test results of both acoustic and aerodynamic measurements are presented and summarized.

3.1. Acoustic measurements

To validate the application for noise reduction, spectrum analysis was performed.

For spectrum analysis, one microphone in the beam-forming array was chosen, located over the tandem rods. The block size was 4096 and data were averaged over 110 blocks. The sound pressure level was referred to 2×10^{-5} Pa.

To begin with, an example was given to pre-analyse the acoustic performance, and more importantly, to find the background noise, e.g. power noise from the main-flow and the plane jet. Figure 9 is an example of the noise spectrum for $L/D = 2$. It is obvious that the three curves overlapped each other within most of the frequency range marked by I, which

could be explained by power noise of the wind tunnel. However, within the frequency range marked by II and III, “PJ” case is noisier than others. Likewise, this noise increase can be explained by power noise from the plane jet generator. Because the acoustic tests were not performed in an anechoic chamber and background noise existed as discussed above, the low frequency part will not be considered in the spectrum analysis below.

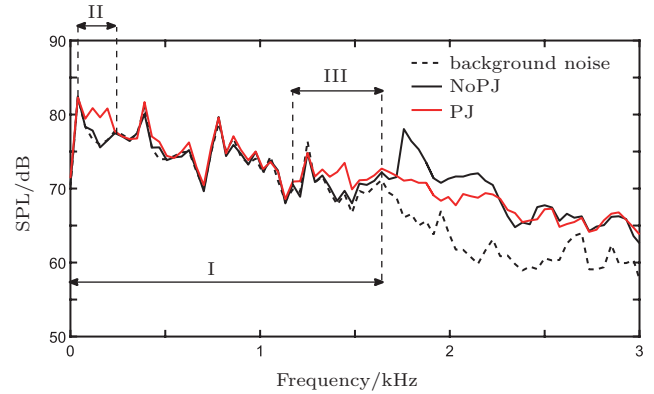


Fig. 9. (color online) Background noise range.

As shown in Fig. 9, “NoPJ” in each case is considerably more noisy than “background noise” and therefore it is concluded that the noise increase is caused by tandem rods. A main tone exists in each regime, approximately in the range of 2 kHz to 2.5 kHz, which is caused by vortex shedding behind the rear rod. The shedding frequency as well as SPL is dependent on L/D . More theory on tandem rods noise generation related to L/D can be found in Refs. [24]–[26]. Additionally, a secondary tone co-exists with the main tone, which can be caused by vortex shedding from the front rod, whose shear layer reattaches alternately, permanently or intermittently onto the rear rod and is weaker. After the plane jet is turned on in “PJ”, overall speaking, noise is notably reduced, especially at both vortex shedding frequencies. It is obvious that the tones are removed by the plane jet. However, for each regime, in some frequency range, the noise in the “PJ” is higher than that in “NoPJ”. This noise increase can be from the plane jet. As is known to all the plane jet can emit jet noise, especially when it interacts with the main-flow. More relevant conclusions would be obtained from noise localization.

Figure 11 is an example of the noise localization by using the beam-forming for $L/D = 3.5$. The contour corresponds to the SPL distribution on the background photo. Data were filtered with the 1/3 octave bands centred at 2 kHz, 4 kHz, 10 kHz, and 16 kHz respectively. Pictures in each column shows comparison between “NoPJ” and “PJ” regimes in the same band, normalized by subtracting the maximum SPL of “NoPJ”. Overall, SPL decreases dramatically after the plane jet is turned on. To be more specific, all the noise localization

results for “NoPJ” clearly illustrate that rods are the main noise source. Nonetheless, the main noise source in “PJ” varies over bands. For bands centered at 2 kHz and 16 kHz, SPL peaks around the plane jet nozzle, which means that the plane jet is the main contributor to noise emission of these bands. By contrast, the main noise source is still tandem rods in bands centered at 4 kHz and 10 kHz. This proves that even with the existence of the plane jet, rods can still make notable noise,

which indicates that there could be further noise reduction potentially.

Figures 12 and 13 respectively illustrate peak reduction at the main shedding frequency and OASPL reduction in certain frequency range with A-weighting, which accounts for relative loudness perceived by human hearing. As is shown, the plane jet works very well for reduction in terms of both tonal and broadband noise.

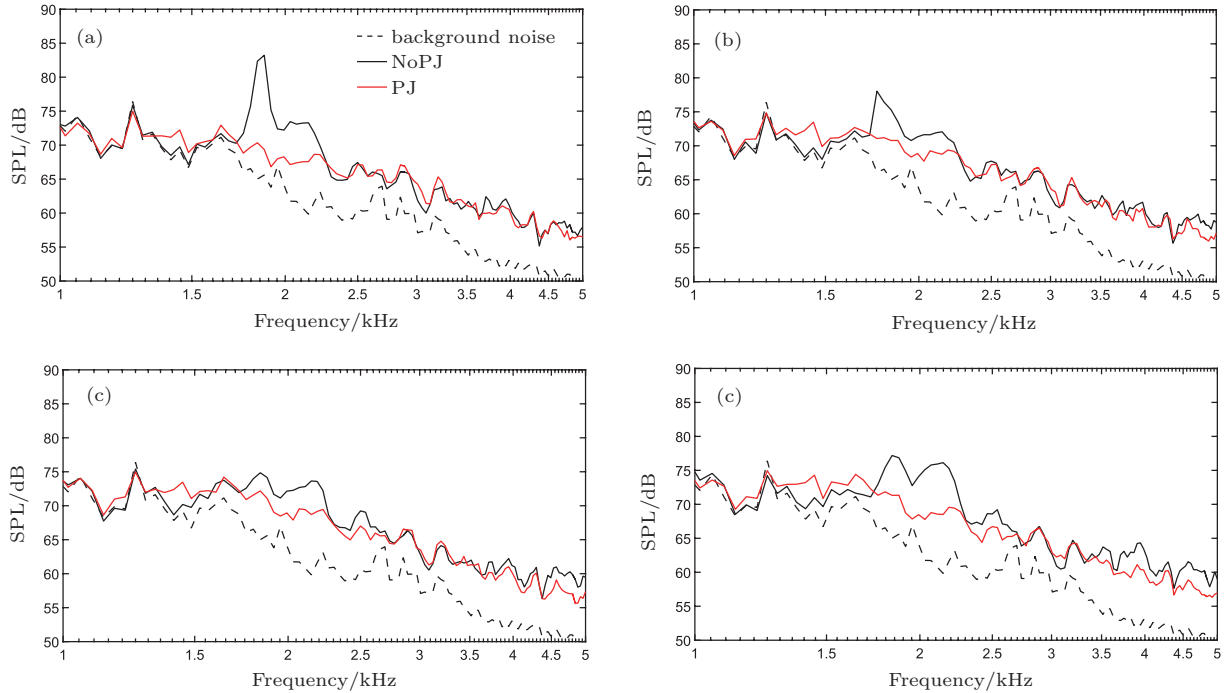


Fig. 10. (color online) Noise spectral of different cases: (a) $L/D = 2$; (b) $L/D = 2.5$; (c) $L/D = 3$; (d) $L/D = 3.5$.

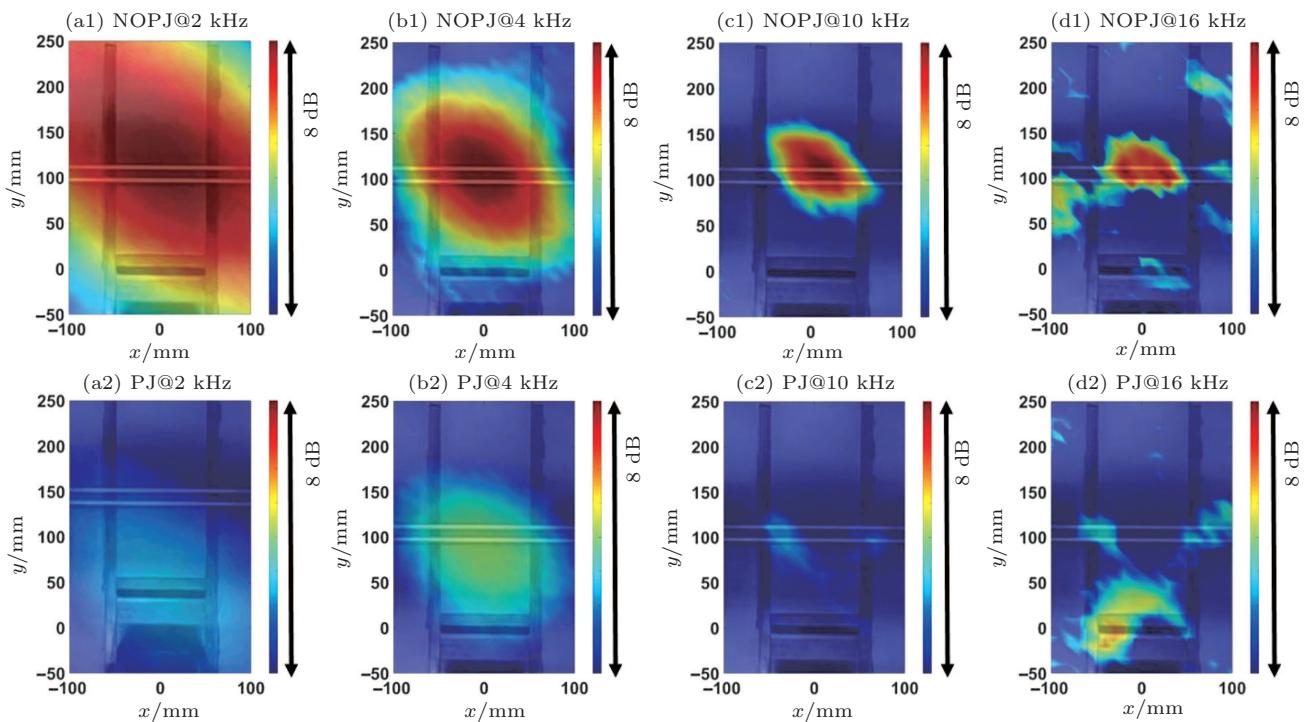


Fig. 11. (color online) Results (case $L/D = 2$) of time domain beam-forming with 1/3 octave band filter centred at: (a) 2 kHz; (b) 4 kHz; (c) 10 kHz; (d) 16 kHz.

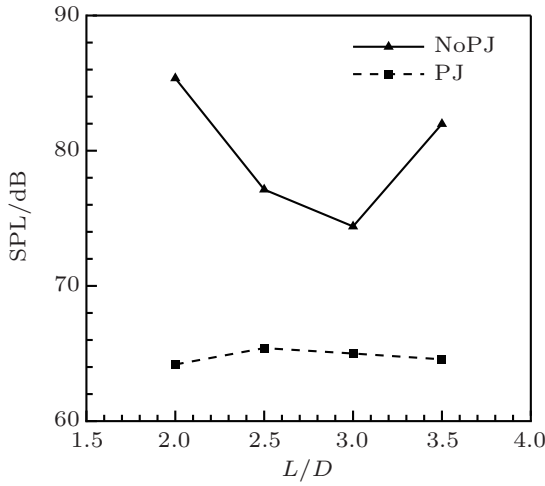


Fig. 12. Peak reduction.

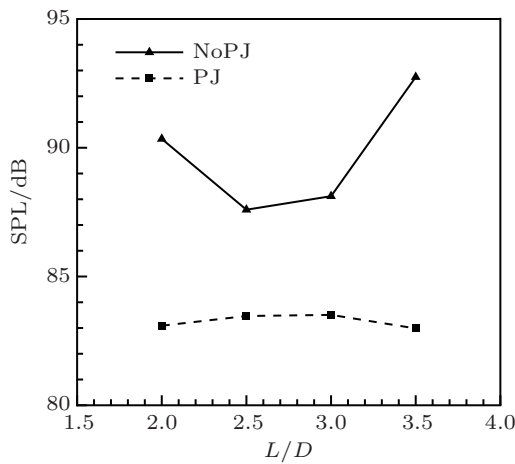


Fig. 13. OASPL reduction.

3.2. Aerodynamics measurements

Figures 14 and 15 present the profiles in the test sections acquired by hot-wire measurement. Height, velocity, and Reynolds stress term are normalized and non-dimensionalised by $D/2$ radius of the rod, U_∞ , and U_∞^2 respectively. As illustrated in Fig. 14(a), all “NoPJ” cases unexpectedly start with lower velocity than “PJ” cases, more precisely, in the range of roughly $0 < 2(h - h_0)/D < 0.7$. The PIV demonstrated that flow speed in the area behind the plane jet can be significantly reduced. Therefore, the reason for slight increase of the flow speed inside the rod gap is unclear. A possible explanation could be recirculation in the wake behind and induced by the front rod.^[27] Hence, further noise generated by rods can be explained by flow coming from behind caused by the recirculation. Subsequently, though velocity profiles of “NoPJ” start from being lower than “PJ”, they soar from around $h = 0.7$ and shortly reach main-flow velocity level, especially around the height of $2(h - h_0)/D = 1$, which is as high as the rod. Moreover, it is at exactly the same height that the vortex shedding happened on the rear rod. By contrast, “PJ” keeps velocity level and does not increase. As acoustic test results already showed, noise of the rods decreased on account of the plane

jet introduction. Therefore, the conclusion can be made that the impinging velocity at $2(h - h_0)/D = 1$ dominates over that of other height in terms of noise generation.

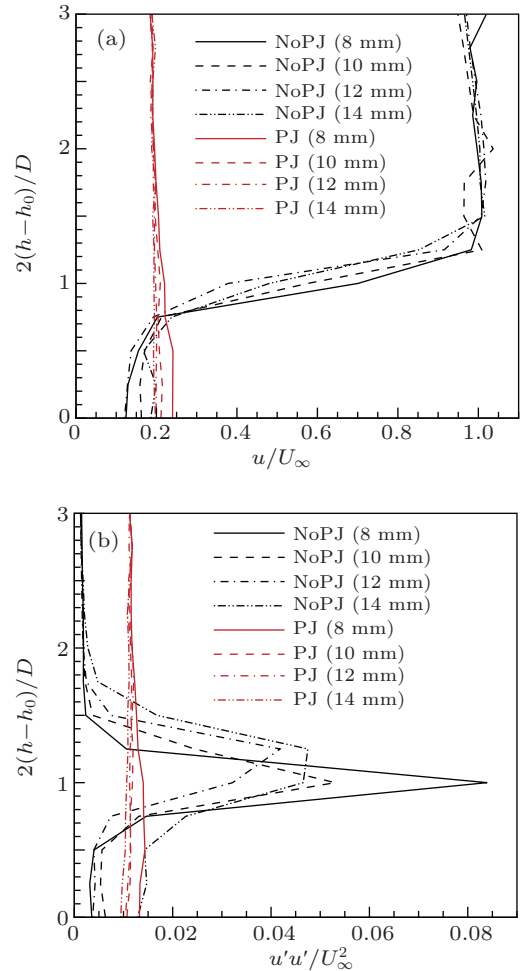


Fig. 14. (color online) Profiles of the test section in front of the rear rod: (a) velocity; (b) Reynolds stress.

Apart from velocity, turbulence level also underlies noise generation. Figure 14(b) depicts Reynolds stress term, which is a sign of turbulence level. Obviously, for all “NoPJ”, $u'u'$ peaks around $0.9 < 2(h - h_0)/D < 1.3$ as a result of shear layer from the front rod and those peaks are eliminated with the existence of the plane jet. Likewise, in the part with low and high height, Reynolds stress in “PJ” is higher than “NoPJ”, which could be possibly attributed to recirculation caused by the front rod as well. Therefore, a similar conclusion can be drawn from a perspective of Reynolds stress, namely impinging turbulence level around $2(h - h_0)/D = 1$ plays a more important role than others in terms of noise generation. Moreover, the plane jet is able to reduce the impinging velocity as well as the turbulence level around this height.

In Fig. 15, i.e., wake of the rear rod, reduction of both u and $u'u'$ are notable with the plane jet on. Specifically, u is significantly reduced at all sampling points. In terms of the Reynolds stress, as shown in Fig. 15(b), in all cases it diminishes in the range of $0 < 2(h - h_0)/D < 1$, which is firmly in-

side the wake of the rear rod. Apparently, it can be concluded that vortex shedding of the rear rod is diminished. With increasing, Reynolds stress in “NoPJ” gradually becomes lower than “PJ”. That is due to the fact that sampling points are outside the wake flow and for those points, turbulence level is higher than “NoPJ” due to the plane jet.

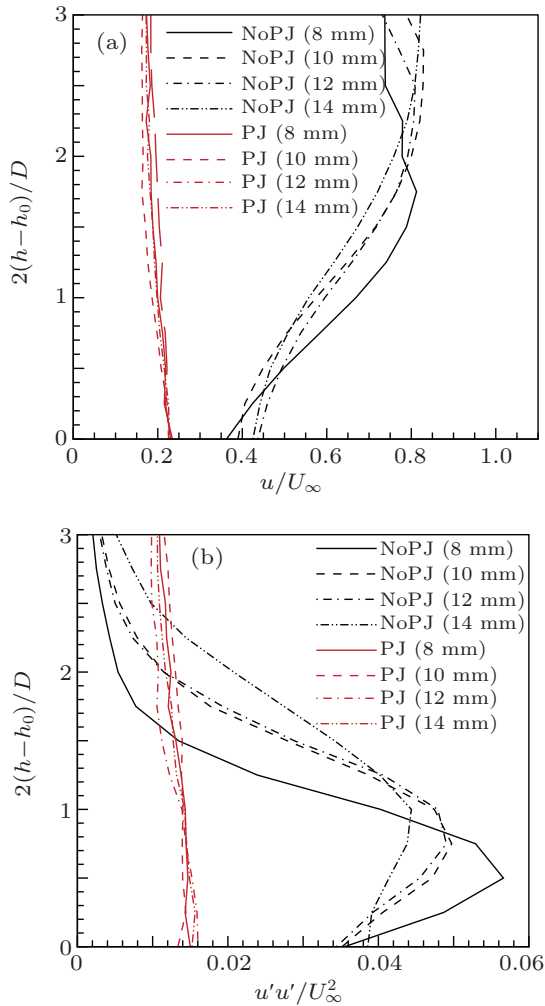


Fig. 15. (color online) Profile of the test section behind the rear rod: (a) velocity; (b) Reynolds stress.

In order to further validate elimination of the vortex shedding induced by the rear rod with the plane jet, velocity fluctuation spectra for “NoPJ” and “PJ” were calculated. Since $2(h-h_0)/D = 1$ is the main shedding place, the analysis was chosen to be at this height. Figure 16 presents the result. Likewise, for noise spectra, the block size was 4096 and the data were averaged over 110 blocks. Here all the fluctuations are referred to U_∞ by dB, i.e.

$$\text{dB} = 20 \log \frac{u'}{U_\infty}. \quad (1)$$

As shown in Fig. 16, fluctuation level stays high in low frequency range that is below around 400 Hz in the spectra of “NoPJ”, then declines with increase of the frequency. A characteristic here is that there are two fluctuation peaks. Those

peaks firmly confirm that the vortex shedding exists behind the rear rod, and the peak in the $L/D = 2$ regime is higher than others, which means that vortex shedding is stronger in 8 mm than others. This is consistent with the noise spectra because tonal noise, i.e. the peak generated in “NoPJ” regime in $L/D = 2$ is also superior to others.

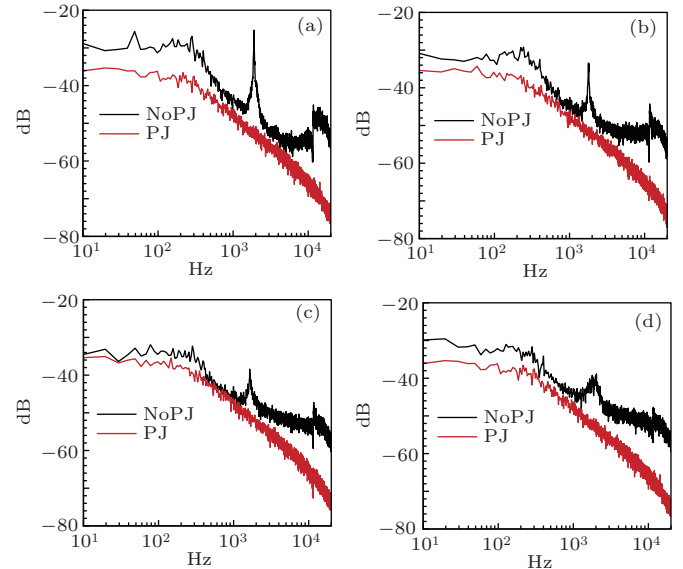


Fig. 16. (color online) Velocity fluctuation spectral at $2(h-h_0)/D = 1$: (a) $L/D = 2$, (b) $L/D = 2.5$, (c) $L/D = 3$, (d) $L/D = 3.5$.

Once the plane jet is turned on, apparently the fluctuation significantly decreases in all frequencies, especially the peaks, as they are removed. These results further demonstrate that the plane jet can potentially be of great use to decrease vortex shedding induced by the rear rod so that noise can be reduced.

4. Conclusions

In this study, acoustic and aerodynamic measurements were conducted in the open-jet wind tunnel on tandem rods noise reduction using the plane jet. In terms of acoustic measurement, test results conclude that the plane jet can be of great use in noise reduction in terms of both tonal and broadband noise. Moreover, the spectra showed that the plane jet itself can emit noise. Noise localization illustrated that the plane jet can subsequently be a main noise source within some frequency ranges whilst in other frequency ranges rods can equally be a main source.

The aerodynamic tests fundamentally explained the reasons for noise reduction. Apart from the fact that the plane jet can reduce the impinging speed to the entire test body, it is also able to reduce turbulence levels of the flow impinging the rear rod at a height equal to that at which vortex shedding takes place. This can help diminish vortex shedding, which is validated by measurements taken behind the rear rod. Both speed and Reynolds stress inside the wake of the rear rod are considerably reduced, so is velocity fluctuation level in spectra.

As a proof-of-concept study, this research indicates the possible application of the plane jet for landing gear noise reduction, especially its usefulness on noise generated by the interaction between the wake of the front component and the rear.

References

- [1] Crighton D G 1991 *Airframe noise* (Cambridge: Cambridge University Press) pp. 391–447
- [2] Macaraeg M, 1998 *4th AIAA/CEAS Aeroacoustics Conference*, June 2–4, 1998, Toulouse, France, 982224
- [3] Li Y, Wang X and Zhang D 2013 *Chinese Journal of Aeronautics* **26** 249
- [4] Nicolas M, Francois P j, Choi C, Malcolm S Werner D and Christelle S 2006 *12th AIAA/CEAS Aeroacoustics Conference*, May 8–10, Cambridge, Massachusetts, 20062623
- [5] Dobrzynski W, Schoning B, Chow L C, Wood C, Smith M and Seror C 2006 *International Journal of Aeroacoustics* **5** 233
- [6] Chow L C, Foot D and Wood C (U.S Patent) 6619587 [2003-09-16]
- [7] Fitzpatrick J 1985 *Journal of Sound and Vibration* **99** 425
- [8] Okolo, P, Zhao, K, Neri, E., Kennedy, J and Bennett, G J 2015 *22nd International Congress on Sound and Vibration*, July 12–16, Florence, Italy
- [9] Li X G, Yang D K and Wang Y 2011 *Chin. Phys. B* **20** 064302
- [10] Chen Y, Huang Y Y, Chen X Q, Bai Y Z and Tan X D 2015 *Chin. Phys. B* **24** 054302
- [11] Zhao K, Neri E, Okolo P, Kennedy J and Bennett G J 2015 *Proceedings of the 22nd International Congress on Sound and Vibration*, July 12–16, Florence, Italy, p. 1414
- [12] Heller H H and Dobrzynski W M 1977 *Journal of Aircraft* **14** 768
- [13] Angland D, Zhang X and Goodyer M 2012 *AIAA Journal* **50** 1670
- [14] Zdravkovich M M 2003 *Flow around Circular Cylinders: Volume 2: Applications* (Oxford: Oxford University Press) pp. 1064–1100
- [15] Eret P and Meskell C 2012 *Advances in Acoustics and Vibration* **2012** 689379
- [16] Robert D 2006 *10th AIAA/CEAS Aeroacoustics Conference*, May 23–25, 2004, Vancouver, British Columbia, Canada, 20042955
- [17] Bruun H H 1996 *Measurement Science and Technology* **7** 10
- [18] Bearman P 1971 *DISA Information* **11** 25
- [19] Kavsaoglu M, Schetz J and Jakubowski A 1989 *Journal of Aircraft* **26** 539
- [20] Ramaprian B 1983 “Turbulence measurements in plane jets and plumes in crossflow”, Ph. D. Dissertation (Iowa Institute of Hydraulic Research, The University of Iowa)
- [21] Jones W and Wille M 1996 *Int. j. heat fluid flow* **17** 296
- [22] Bhattacharyya K and Pop I 2014 *Chin. Phys. B* **23** 024701
- [23] Ishak A, Nazar R and Pop I 2007 *Chin. Phys. Lett.* **24** 2274
- [24] Hutcheson F and Brooks T 2012 *International Journal of Aeroacoustics* **11** 291
- [25] David L, Mehdi K, Meelan C, Florence H, Thomas B, Daniel S 2007 *13th AIAA/CEAS Aeroacoustics Conference*, May 21–23, 2007, Rome, Italy, 20073450
- [26] Luther J, Mehdi K, Meelan C and Cathy M 2005 *11th AIAA/CEAS Aeroacoustics Conference*, May 23–25, Monterey, California, USA, 20052812
- [27] Williamson C H 1996 *Ann. Rev. Fluid Mech.* **28** 477